

Online Hybrid Zero Dynamics Optimal Gait Generation Using Legendre Pseudospectral Optimization

Ayonga Hereid¹, Shishir Kolathaya¹ and Aaron D. Ames²

Abstract—This paper presents an optimal gait synthesis method that exploits the full body dynamics of robots using the Hybrid Zero Dynamics (HZD) control framework—for the first time—experimentally realizes online HZD gait generation for a planar underactuated robot. Hybrid zero dynamics is an established theoretical framework that formally enables stable control of dynamic locomotion by enforcing virtual constraints through feedback controllers. An essential part of successfully realizing dynamic walking with HZD framework is determining parameters of the virtual constraints that satisfy hybrid invariant condition via nonlinear constrained optimization. Due to the complexity of the full hybrid system model of the robot, these optimization problems often suffer from slow convergence and local minima. In this paper, we improve the reliability of the HZD gait optimization and significantly increase the convergence speed by taking advantage of the direct transcription formulation and the exponential convergence of the global orthogonal collocation (a.k.a. pseudospectral) method. As a result, generating of HZD gaits online becomes feasible with an average computation time less than 0.5 seconds, as will be demonstrated experimentally on a bipedal robot.

I. INTRODUCTION

The goal of bipedal robots is to demonstrate dynamic and agile locomotion that allows for navigation of terrain not approachable by wheeled robots. Yet the ability to accommodate changes in terrain present in uncontrolled environments, however, is a challenging problem. The difficulty arises from the fact that planning dynamic motions that are consistent to the full body dynamics of the complex robot model is often computationally expensive. This paper presents a novel optimization formulation which enables existing nonlinear programming (NLP) solvers to generate dynamic gaits online within the HZD framework, and experimentally evaluated this method on an underactuated planar robot, DURUS-2D.

Existing methods of motion planning typically use reduced-order models, such as the linear inverted pendulum model (LIPM) [14], to mitigate the complexity of full body dynamics. By balancing the robot about the Zero Moment Point (ZMP) [22], these approaches plan trajectories for the simplified model and then generate the whole body motion by conforming the robot to these analytically tractable dynamics [15], [17]. These simplifications, however, place stringent requirements on the design of the robot (e.g. all

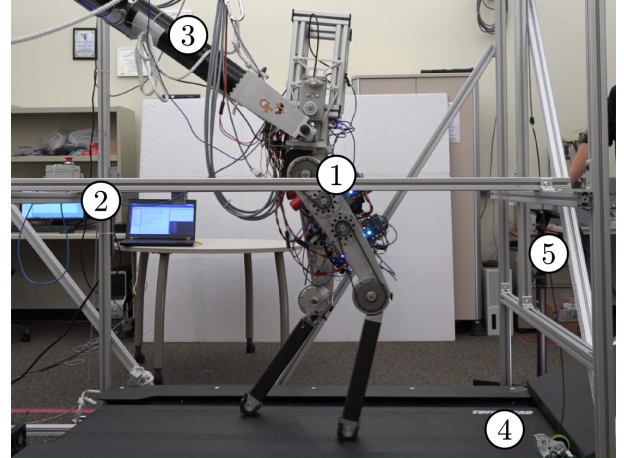


Fig. 1: Experimental setup of the DURUS-2D walking on a treadmill. The labels represent: (1) DURUS-2D robot, (2) the control workstation, (3) the linear boom used to constrain DURUS-2D to the sagittal plane, (4) the treadmill whose actual velocity is measured by an encoder attached, (5) the control panel used to change the velocity of the treadmill.

joints must be actuated with no significant compliance) and restrictions on the overall locomotion capabilities of the machine (e.g. the robot must always walk with a constant center-of-mass height). Embracing planning and formal control that exploits the full body dynamics of the robot is a path toward unlocking the fully dynamic capabilities of the machine. An increasing number of methods have been developed to generate optimal gaits using full-body dynamics optimization [16], [18]. Some researchers also explore a middle path, in which whole body motion is planned with the robot’s centroidal dynamics subject to full body kinematic constraints [6]. While these methods can realize more dynamic behaviors, the optimizations require excessive amount of time to run and may not be able to converge reliably, and therefore, are only suitable for off-line *a priori* motion planning.

Hybrid zero dynamics (HZD) [24] is a formal framework that utilizes the full-order dynamics of the hybrid system model by synthesizing feedback controllers that yield periodic dynamic locomotion even in the presence of underactuation [4], [12], [21] and multi-contact foot behaviors [25]. In the HZD framework, a set of *virtual constraints* enforced via nonlinear feedback controllers, formally yielding a low-dimensional representation of the system which captures the stability properties of full-order dynamics if the virtual constraints are invariant through impact. Hence the planning of

This research is supported by DARPA grant D15AP00006 and NSF grants CPS-1239055 and NRI-1526519.

¹Ayonga Hereid and Shishir Kolathaya are with the Woodruff School of Mechanical Engineering, Georgia Institute of Technology, Atlanta, GA, 30332 USA

²Aaron D. Ames is with the Woodruff School of Mechanical Engineering and the School of Electrical and Computer Engineering, Georgia Institute of Technology, Atlanta, GA, 30332 USA

HZD gaits can be transformed into a nonlinear optimization that determines the parameters of virtual constraints satisfying a hybrid invariance condition. However, existing methods for generating such gaits are often time-consuming, and thus must be performed off-line. While advanced control methods [3], [11] have been developed to robustify the gait under perturbations and switch between gaits (often encoded as *motion primitives*) [19], these methods are restricted to a limited number of gaits generated in advance.

In this paper, we present an online HZD gait generation method using the *pseudospectral* optimization formulation. Exploiting the advantages of direct transcription formulation of the pseudospectral method, we formulate the HZD gait optimization in a fashion that makes it amendable to being solved in a fast and reliable fashion utilizing existing NLP solvers. More importantly, the proposed approach opens the possibility of generating optimal gaits online while considering the whole body dynamics of the robot. We experimentally evaluate the performance of this method on a planar underactuated robot which walks on a treadmill with varying speeds. As a result, the optimizer successfully generates gaits with different walking speeds online to enable the robot to adjust to the changing speed of the treadmill—this provides the first example of online HZD gait generation.

II. HYBRID ZERO DYNAMICS FRAMEWORK

This section will focus on the *hybrid zero dynamics* (HZD) control framework that will be utilized to achieve stable periodic orbits in systems with impact. The formal definitions in this section provide the necessary structure for formulating the fast HZD gait optimization problem.

A. Bipedal Walking as a Hybrid System

Dynamic bipedal locomotion is often modeled as a hybrid control system in literature, wherein walking consists of an alternating sequence of continuous and discrete events [2], [10]. We will consider an example robot, the 5-link underactuated planar robot, DURUS-2D, to simplify the construction of the hybrid system model. As shown in Fig. 2a, (p_x, p_z, q_{sf}) represents the Cartesian position of stance foot and the angle of stance calf with respect to fixed inertia frame respectively, and $(q_{sk}, q_{sh}, q_{nsh}, q_{nsk})$ represent the actuated joints: stance knee, stance hip, non-stance hip and non-stance knee, respectively. The floating base coordinates of planar DURUS-2D then can be given as, $q = (p_x, p_z, q_{sf}, q_{sk}, q_{sh}, q_{nsh}, q_{nsk}) \in \mathcal{Q}_R \subset \mathbb{R}^7$. Let \mathcal{Q} be the configuration space of the robot with coordinates $q \in \mathcal{Q}$, the *hybrid control system* is given as a tuple [2],

$$\mathcal{HC} = (\mathcal{D}, \mathcal{U}, S, \Delta, FG), \quad (1)$$

where $\mathcal{D} \subseteq T\mathcal{Q} \times \mathcal{U}$ is an admissible domain, $\mathcal{U} \subseteq \mathbb{R}^4$ is a set of admissible controls, $S \subset \mathcal{D}$ is a *guard* that determines the switching surface of discrete events, $\Delta : \pi(S) \rightarrow \pi(\mathcal{D})$ is a smooth *reset map* with $\pi : \mathcal{D} \rightarrow T\mathcal{Q}$ a canonical projection, and *FG* is the affine control system defined on \mathcal{D} , i.e., $\dot{x} = f(x) + g(x)u$ with $(x, u) \in \mathcal{D}$ and $u \in \mathcal{U}$, where $x = (q, \dot{q})$ is the set of states.

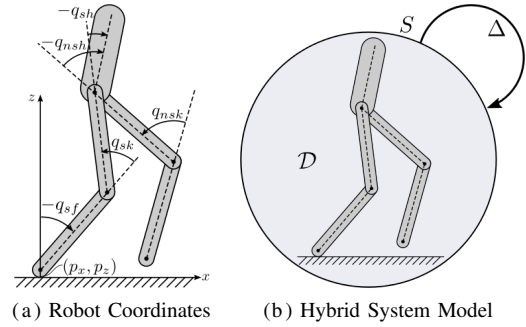


Fig. 2: Model configuration of the DURUS-2D robot.

Continuous Dynamics. The continuous dynamics is given by the Lagrangian and the foot kinematic constraints with the ground. During the continuous event (swinging of the non-stance leg), the normal ground reaction forces constrain the foot to the ground, i.e., $\eta(q) = (p_x, p_z) \equiv \text{constant}$. To satisfy the contact constraints, the second order differentiation should be zero. That is,

$$J(q)\ddot{q} + \dot{J}(q, \dot{q})\dot{q} = 0, \quad (2)$$

with $J(q) = \frac{\partial \eta(q)}{\partial q}$. With the mass, inertia and length properties of each link of the planar DURUS-2D model, the constrained continuous dynamics of the system can be determined by the classical Euler-Lagrange equation [10]:

$$D(q)\ddot{q} + H(q, \dot{q}) = Bu + J^T(q)F, \quad (3)$$

where $D(q)$ is the inertia matrix, $H(q, \dot{q}) = C(q, \dot{q})\dot{q} + G(q)$ is the vector containing the Coriolis, centrifugal and the gravity terms, B is the actuator distribution matrix, and $F : T\mathcal{Q} \times U \rightarrow \mathbb{R}^2$ is a vector of ground reaction forces. The reaction forces $F(q, \dot{q}, u)$ can be determined from (3) and (2), yielding the affine control system *FG*.

Domain of Admissibility. The admissible conditions of the domain \mathcal{D} is determined by unilateral constraints of the system. For example, the foot contact is considered to be a unilateral constraint. The reaction forces must satisfy the friction cone constraints and the normal force should be positive. In addition, the non-stance foot must be above the ground throughout a step. We formulate these conditions in terms of inequalities, given as

$$A(q, \dot{q}, u) = \begin{bmatrix} \mathcal{R}F(q, \dot{q}, u) \\ h_{nsf}(q) \end{bmatrix} \geq 0, \quad (4)$$

where \mathcal{R} is a constant matrix capturing the friction cone and the positive normal force constraints. Hence, the domain of admissibility is defined as:

$$\mathcal{D} = \{(q, \dot{q}, u) \in T\mathcal{Q} \times U | A(q, \dot{q}, u) \geq 0\}. \quad (5)$$

The guard $S \subset \mathcal{D}$ at which the discrete event occurs is a co-dimensional one submanifold of the domain. Let $h : \mathcal{D} \rightarrow \mathbb{R}$ be an appropriate element of (4) associated with the discrete event, the guard is defined as

$$S = \{(q, \dot{q}, u) \in \mathcal{D} | h(q, \dot{q}, u) = 0, \dot{h}(q, \dot{q}, u) < 0\}. \quad (6)$$

For the walking of DURUS-2D, this switching surface is defined when the height of the non-stance foot crosses zero, i.e., $h(q) = h_{nsf}(q)$.

Discrete Dynamics. A discrete event occurs when the non-stance foot hits the ground. We assume the impact is perfectly plastic [13]. While configurations of the system are invariant through the impact, i.e., $q^+ = q^-$, post-impact velocities must satisfy the plastic impact equation:

$$\begin{bmatrix} D(q) & -J^T(q) \\ J(q) & 0 \end{bmatrix} \begin{bmatrix} \dot{q}^+ \\ \delta F \end{bmatrix} = \begin{bmatrix} D(q)\dot{q}^- \\ 0 \end{bmatrix}, \quad (7)$$

where δF are impulsive forces. Solving (7), we get

$$\dot{q}^+ = P(q, \dot{q}^-) = (I - D^{-1}J^T(JD^{-1}J^T)^{-1}J)\dot{q}^-, \quad (8)$$

where I is an identity matrix. This yields the reset map

$$(q^+, \dot{q}^+) = \Delta(q^-, \dot{q}^-) = \begin{bmatrix} \mathcal{R}q^- \\ \mathcal{R}P(q, \dot{q}^-) \end{bmatrix}, \quad (9)$$

where \mathcal{R} is the relabeling matrix that swaps the left and the right leg at every step [2].

B. Hybrid Zero Dynamics

In the hybrid zero dynamics framework, virtual constraints are introduced as a means to synthesize feedback controllers that realize stable and robust locomotion in underactuated robots. By designing virtual constraints that are invariant through impact, an invariant submanifold is created—termed the *hybrid zero dynamics surface*—wherein the evolution of the system is dictated by the low-dimensional hybrid dynamical system [2], [24]. The focus of this subsection is to derive conditions under which hybrid zero dynamics can be realized in the bipedal robot.

Virtual Constraints. Virtual constraints are defined as the difference between the actual and the desired outputs of the robot:

$$y_2 = y_2^a(q) - y_2^d(\theta, \alpha), \quad (10)$$

where y_2 is (vector) relative degree 2 by definition. In this paper, we pick actuated joint angles as our actual outputs,

$$y_2^a(q) = (q_{sk}, q_{sh}, q_{nsh}, q_{nsk}). \quad (11)$$

Desired outputs, y_2^d , are defined in terms of 5-th order Bézier polynomials parameterized by α and θ is a strictly monotonic state-based parameterization of time.

Feedback Controller. With the goal of driving the virtual constraints $y_2 \rightarrow 0$ exponentially, we consider the feedback linearization control law:

$$u^{(\alpha, \varepsilon)} = -(L_g L_f y_2)^{-1} (L_f^2 y_2 + 2\varepsilon L_f y_2 + \varepsilon^2 y_2) \quad (12)$$

with a control gain $\varepsilon > 0$, where L_f and L_g are Lie derivatives. Applying this control law to the hybrid control system in (1) results in linear output dynamics:

$$\dot{y}_2 = -2\varepsilon L_f y_2 - \varepsilon^2 y_2. \quad (13)$$

This yields a *hybrid system* of (1) with $\mathcal{U} = \{\emptyset\}$, given as,

$$\mathcal{H}^{(\alpha, \varepsilon)} = (\mathcal{D}^X, S^X, \Delta, F^{(\alpha, \varepsilon)}), \quad (14)$$

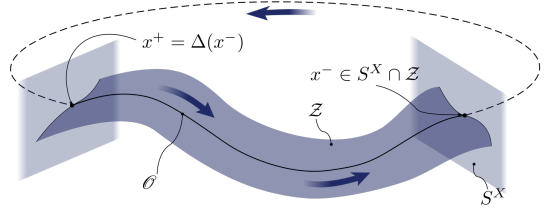


Fig. 3: A periodic orbit on the Hybrid Zero Dynamics surface

where $\mathcal{D}^X \subset TQ$ is an admissible domain, S^X is a *guard* with $S^X \subset \mathcal{D}^X$, and $F^{(\alpha, \varepsilon)}$ is a dynamical system defined on \mathcal{D}^X , i.e., $\dot{x} = f^{(\alpha, \varepsilon)}(x) = f(x) + g(x)u^{(\alpha, \varepsilon)}$ with $x \in \mathcal{D}^X$.

Periodic Orbit. For the hybrid system $\mathcal{H}^{(\alpha, \varepsilon)}$, let $\varphi_t(x)$ be a flow of the continuous dynamics $F^{(\alpha, \varepsilon)}$ in (14). For $x^* \in S$, we say that $\varphi_t(x)$ is hybrid periodic if there exists a finite $T > 0$ such that $\varphi_T(\Delta(x^*)) = x^*$. A set $\mathcal{O} \subset \mathcal{D}^X$ is a hybrid periodic orbit if $\mathcal{O} = \{\varphi_t(\Delta(x^*)) : 0 < t < T\}$ for a hybrid periodic flow $\varphi_t(x)$ (see Fig. 3). Further, x^* is the fixed point, if the periodic orbit \mathcal{O} is *transversal* to S^X in exactly one point x^* . For the stability of periodic orbits in the context of Lyapunov, we refer the readers to [3].

Hybrid Zero Dynamics. With the feedback control law in (12), the *zero dynamics* submanifold,

$$\mathcal{Z} = \{(q, \dot{q}) \in TQ | y_2 = 0, \dot{y}_2 = 0\}. \quad (15)$$

is rendered invariant in the continuous domain. However, it is not necessarily invariant through discrete dynamics without carefully designing the virtual constraints. Therefore, if there exist a set of parameters α so that the submanifold \mathcal{Z} is impact invariant, i.e.,

$$\Delta(x) \in \mathcal{Z}, \quad \forall x \in S \cap \mathcal{Z}, \quad (16)$$

then we call \mathcal{Z} the *hybrid zero dynamics surface*. That is, any solution that starts in \mathcal{Z} remains in \mathcal{Z} , inspite of the impacts in \mathcal{Z} , see Fig. 3. As a result, the behavior on this reduced-dimensional space can be used to encode the full-order behavior of the bipedal humanoid robot. Therefore, the goal is to find a set of parameters α that satisfies the HZD constraints in (16). Importantly, the end result is a means of formally encoding and realizing dynamic walking gaits.

III. ONLINE HZD GAIT OPTIMIZATION

This section will focus on obtaining a novel HZD gait optimization formulation for underactuated robots subject to the hybrid zero dynamics framework. Utilizing the pseudospectral method with a novel modification via the introduction of defect variables, we present a computationally fast and reliable optimal gait generation method. These methods will form the basis for the experimental realization of online gait generation.

The prevailing approaches to generate hybrid zero dynamics gaits are via *direct single shooting* methods. In some particular cases, the closed form solution of the zero dynamics can be obtained analytically, and the HZD constraints in (16) can be stated as algebraic constraints. This fact has been

successfully taken advantage of in such *direct single shooting* methods to generate HZD gaits for fully actuated robots [19] and planar point-feet robots [2]. However, the integration of the full order dynamics is inevitable for checking physical constraints and specific objective-oriented constraints, e.g., the walking speed. The complexity of constraint expressions in such a formulation significantly impedes its performance even for relatively simpler planar robot models.

In this paper, we employ the global orthogonal collocation—often termed as *pseudospectral methods*—in which the time-marching forward integration of system dynamics is replaced with algebraic collocation equalities at particular collocation nodes [7]. The end result is a nonlinear programming problem. In addition, this formulation enables the use of defect variables by which the constraint expressions can be further simplified, so that the analytical Jacobian, even Hessian, of the optimization problem can be determined.

A. Legendre Pseudospectral Method

In the Legendre pseudospectral method, the basic idea is to approximate the solution of the dynamical system by N -th order Lagrange interpolating polynomials which interpolate the solutions at Legendre-Gauss-Lobatto (LGL) nodes. The LGL nodes are defined as zeros of $(\tau^2 - 1)\dot{L}_N(\tau)$ distributed on the interval $\tau \in [-1, 1]$, where $\dot{L}_N(\tau)$ is the derivative of the N -th order Legendre polynomial $L_N(\tau)$ [9]. Let $x_i = (q_i, \dot{q}_i)$ be approximated states at node τ_i , then the solution $x(\tau)$ on $\tau \in [-1, 1]$ is approximated by

$$x(\tau) \approx \bar{x}(\tau) = \sum_{i=0}^N x_i \phi_i(\tau) \quad (17)$$

where $\phi_i(\tau) = \frac{1}{N(N+1)L_N(\tau_i)} \frac{(\tau^2 - 1)\dot{L}_N(\tau)}{\tau - \tau_i}$ is the Lagrange interpolating polynomial of order N . It can be noted that $\phi_i(\tau_k) = 1$, if $i = k$ and $\phi_i(\tau_k) = 0$ if $i \neq k$. Similarly, the derivate of $x(\tau)$ is approximated by differentiating the approximation $\bar{x}(\tau)$ in (17),

$$\dot{x}(\tau) \approx \dot{\bar{x}}(\tau) = \sum_{i=0}^N x_i \dot{\phi}_i(\tau). \quad (18)$$

Interestingly, the derivative of $\phi_i(\tau_k)$ at any LGL node τ_k is a constant determined only by i and k , given by [20]:

$$\dot{\phi}_i(\tau_k) = \begin{cases} \frac{L_N(\tau_i)}{L_N(\tau_k)(\tau_i - \tau_k)}, & \text{if } i \neq k, \\ -\frac{N(N+1)}{4}, & \text{if } i = k = 0, \\ \frac{N(N+1)}{4}, & \text{if } i = k = N, \\ 0, & \text{otherwise.} \end{cases} \quad (19)$$

The collocation condition is defined such that at all LGL nodes the approximated derivatives in (18) equal to the derivatives that are computed from the system dynamics. By using global orthogonal polynomials which interpolate at orthogonally collocated points, the pseudospectral method provides an approximation of the solution that has exponential convergence (as a rate of the number of LGL nodes) to the smooth solution [20].

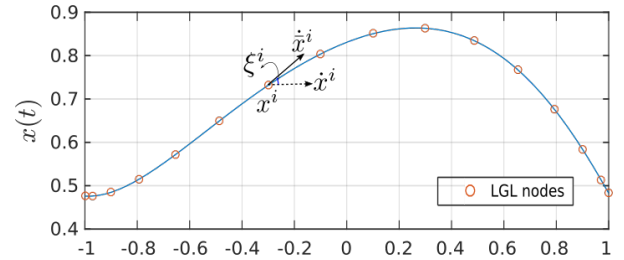


Fig. 4: Demonstration of the global orthogonal collocation using Legendre-Gauss-Lobatto (LGL) points.

B. HZD Gait Optimization

The goal of hybrid zero dynamics gait optimization is to find a set of parameters α so that the system in (14) has a hybrid periodic orbit and satisfy the hybrid invariance condition stated in (16). We start with stating collocation constraints particularly for the periodic solution of the hybrid system in (14). In particular, we consider a hybrid periodic orbit \mathcal{O} with period T . Note that the Legendre interpolating polynomials are defined on the interval $[-1, 1]$, which can be transformed to the time interval $[0, T]$ via the affine transformation, i.e., $t = \frac{T}{2}(\tau + 1)$ [8].

Let $\bar{\mathcal{O}} = \{(q_k, \dot{q}_k) \in \mathcal{O} : k \in \mathbb{N} \text{ and } 0 \leq k \leq N\}$ be a set of discretized states of a periodic orbit \mathcal{O} at N -th-order LGL nodes, the hybrid zero dynamics gait optimization problem can be stated to find a set of optimal parameters α^* that satisfies the HZD condition in (16) while minimizing a cost function Φ :

$$(\bar{\mathcal{O}}^*, \alpha^*, T^*) = \underset{(\bar{\mathcal{O}}, \alpha, T)}{\operatorname{argmin}} \Phi(\bar{\mathcal{O}}, \alpha, T) \quad (20)$$

$$\text{s.t. } \sum_{i=0}^N x_i \dot{\phi}_i(\tau_k) - \frac{T}{2} f^{\alpha, \varepsilon}(x_k) = 0, \quad (C1)$$

$$A(x_k, u^{(\alpha, \varepsilon)}(x_k)) \geq 0, \quad (C2)$$

$$h(x_N) = 0, \quad \dot{h}(x_N) < 0, \quad (C3)$$

$$\Delta(x_N) \in \mathcal{Z}, \quad x_0 - \Delta(x_N) = 0. \quad (C4)$$

for all $k \in \{0, 1, \dots, N\}$, where the collocation constraint (C1) determines that the (approximated) states x_k are indeed solutions of the continuous dynamics $F^{(\alpha, \varepsilon)}$, (C2) guarantees that the solution always lies in the domain manifold, (C3) ensures that $x_N \in S$, and (C4) satisfies the hybrid invariance condition in (16) and the solution is periodic.

C. Defect Variables Formulation for Fast Optimization

Solving the problem in (20) results in a periodic walking gait that has HZD. However, some constraints are still too complicated to compute their analytical Jacobian directly. In particular, calculating the continuous dynamics, the reset map and the feedback controllers require inverting matrices, which is extremely expensive for symbolic computation.

Defect variables are supplementary decision variables that could be computed in closed-form initially. Introducing defect variables will significantly simplify the constraint

expression so that determining the analytical Jacobian of constraints becomes feasible [12]. In nonlinear programming problems, providing analytical Jacobian of constraints would significantly increase the computation speed and improve the robustness of the optimization convergence. Hence, in addition to $\bar{\mathcal{O}}$, α and T , we define a set of defect variables at each node $\bar{\mathcal{Z}} = \{(\ddot{q}_k, u_k, F_k) : k \in \mathbb{N} \text{ and } 0 \leq k \leq N\}$, the impact impulsive forces δF at the last node.

Now we re-formulate the constraints of the optimization problem (20) with defect variables. In particular, the computation of closed-loop system dynamics can be stated in terms of $\dot{x}_k = (\dot{q}_k, \ddot{q}_k)$ directly, i.e.,

$$\sum_{i=0}^N x_i \dot{\phi}_i(\tau_k) - \frac{T}{2} \dot{x}_k = 0, \quad (\text{C1-a})$$

for all $j \in \{0, 1, \dots, N\}$. Additional equality constraints must be imposed so that \dot{x}_k indeed satisfy the closed-loop dynamics. Here we use the approach in [12], in which the constrained Lagrangian dynamics equation in (3), holonomic constraints in (2), and output dynamics in (13) are imposed to equivalently (and fully) represent the closed loop dynamics $f^{(\alpha, \varepsilon)}(x)$. Thus, we have following equalities:

$$D(q_k)\ddot{q}_k + H(q_k, \dot{q}_k) - Bu_k - J^T(q_k)F_k = 0, \quad (\text{C1-b})$$

$$J(q_k)\ddot{q}_k + \dot{J}(q_k, \dot{q}_k)\dot{q}_k = 0, \quad (\text{C1-c})$$

$$\begin{aligned} \ddot{y}_2(q_k, \dot{q}_k, \ddot{q}_k, \alpha) + 2\varepsilon \dot{y}_2(q_k, \dot{q}_k, \alpha) + \\ \varepsilon^2 y_2(q_k, \alpha) = 0, \end{aligned} \quad (\text{C1-d})$$

for all $k \in \{0, 1, \dots, N\}$. It can be noted that the holonomic constraints in (C1-c) determines the constraint wrenches when coupled with (C1-b), and (C1-d) determines u_k implicitly without the explicit calculation of the feedback control law given in (12). The result is a set of smooth control inputs that drives $y_2 \rightarrow 0$ given $\varepsilon > 0$. The modification of (C2) is straightforward considering the fact that u_k is now part of the decision variables taken into account. More importantly, constraints of reaction forces in (4) now can be stated directly in terms of F_k . For all $k \in \{0, 1, \dots, N\}$, we have

$$A(x_k, u_k, F_k) \geq 0 \quad (\text{C2-a})$$

Similarly, instead of using the reset map given in (9) for the constraints (C4), we enforce equality constraints in terms of the impact equation given in (7). Moreover, the hybrid invariance constraints can be directly imposed on the states at the first node.

$$q_0 - \mathcal{R}q_N = 0, \quad (\text{C4-a})$$

$$J(q_0)\mathcal{R}\dot{q}_0 = 0, \quad (\text{C4-b})$$

$$D(q_0)(\dot{q}_0 - \mathcal{R}\dot{q}_N) - J^T(q_0)\delta F = 0, \quad (\text{C4-c})$$

$$y_2(q_0, \alpha_0) = 0, \quad (\text{C4-d})$$

$$\dot{y}_2(q_0, \dot{q}_0, \alpha_0) = 0. \quad (\text{C4-e})$$

In addition, the contact constraints must equal the desired constants (for DURUS-2D walking, the constants are zero):

$$\eta(q_0) = 0 \quad (\text{C4-f})$$

With these modified constraints, we are able to rigorously compute analytical expressions of the gradient of the cost function and the Jacobian of the constraints, even the Hessian of the optimization problem [23], using any proper symbolic mathematics software. The end result is a fast and reliably converging nonlinear programming problem for generating dynamic walking gaits for the DURUS-2D robot within the hybrid zero dynamics framework.

IV. SPEED REGULATION VIA ONLINE OPTIMAL GAIT GENERATION

In this section, we employ the gait generation formulation to design optimal gaits online. In particular, we optimize new HZD gaits subject to a specific desired forward velocity that changes when the robot is still walking, and apply the newly optimized gait parameters α^* to change the walking velocity of the robot in real time.

Objective-Oriented Constraints. We start with formulating objective-oriented (OC) constraints for this particular purpose. For periodic walking gait, the distance travelled during a step equals the step length of the gait. Let \bar{v}^d be the desired forward speed of the robot, the optimized gait should satisfy the following condition:

$$\left\| \frac{L_{step}(q_N)}{T} - \bar{v}^d \right\| \leq \delta \quad (\text{OC1})$$

for a small constant $\delta > 0$, where $L_{step}(q_N) = p_{nsf}^x(q_N)$ is the step length and $p_{nsf}^x(q)$ is the x -position of the non-stance foot. With a goal to apply optimized gaits to the robot hardware on the fly, additional constraints must be enforced so that the resulting gaits are reasonable and feasible from the viewpoint of the actual hardware. In particular, we consider the following constraints.

- The upper body should be upright as much as possible, i.e., given $q_{tor}(q) = -q_{sf} - q_{sk} - q_{sh}$,

$$q_{tor}^{\min} \leq q_{tor}(q) \leq q_{tor}^{\max}. \quad (\text{OC2})$$

- There should be enough swing foot clearance to prevent scuffing, which we constrain in such a way that the non-stance foot is always above a predetermined curve:

$$h_{nsf}(q) - h_{nsf}^d(s(q)) \geq 0, \quad (\text{OC3})$$

where $h_{nsf}^d(s(q))$ is the desired foot clearance curve.

- The joint velocities and actuator torques must be within the specifications of the motors:

$$-\dot{q}^{\max} \leq \dot{q} \leq \dot{q}^{\max}, \quad (\text{OC4})$$

$$-u^{\max} \leq u \leq u^{\max}. \quad (\text{OC5})$$

Energy Efficient Gait Optimization. With a goal to achieve energy efficient locomotion at a specific speed, the cost function of the NLP is defined as the mechanical cost of transport of the gait, given as:

$$\Phi(\bar{\mathcal{O}}, \bar{\mathcal{Z}}) := \frac{1}{mgL_{step}(q_N)} \sum_{k=0}^N w_k P(u_k, \dot{q}_k) \quad (21)$$

where w_k 's are the LGL weights given by

$$w_k = \frac{2}{N(N+1)} \frac{1}{L_N(\tau_k)^2}, \quad (22)$$

and $P(u, \dot{q})$ is the total power of the actuated joints:

$$P(u, \dot{q}) = \|u \circ (B^T \dot{q})\|^2, \quad (23)$$

considering positive and negative powers [5]. Let $\mathbf{Z} = \{\bar{\mathcal{O}}, \alpha, T, \bar{\mathcal{X}}, \delta F\}$ be the set of augmented decision variables, and $\mathbf{C}(\mathbf{Z})$ as a vector of constraints given in (C1)–(C4)¹ and (OC1)–(OC5), we state the speed regulation gait optimization problem as,

$$\begin{aligned} \mathbf{Z}^* &= \underset{\mathbf{Z}}{\operatorname{argmin}} \Phi(\mathbf{Z}) \\ \text{s.t.} \quad \mathbf{C}^{\min} &\leq \mathbf{C}(\mathbf{Z}) \leq \mathbf{C}^{\max} \\ \mathbf{Z}^{\min} &\leq \mathbf{Z} \leq \mathbf{Z}^{\max} \end{aligned} \quad (24)$$

where \mathbf{Z}^{\min} and \mathbf{Z}^{\max} are the minimum and maximum values of the decision variables, and \mathbf{C}^{\min} and \mathbf{C}^{\max} are the vectors containing the minimum and maximum values of constraints, respectively. For equality constraints, the corresponding minimum and maximum values in \mathbf{C}^{\min} and \mathbf{C}^{\max} are both set to zero. This HZD gait generation NLP is then solved using IPOPT [23] with linear solver ma57.

V. EXPERIMENTAL RESULTS

In this section, we present the experimental results of the online speed regulation optimization that we have proposed in the previous section.

Experimental Setup. As shown by Fig. 1, the robot is mounted on the treadmill utilizing a cage on which a boom is mounted. The robot is constrained to the lateral plane to restrict the robot to up-down and forward-backward movements only—that is, the boom *only* supports the robot in the lateral plane. The boom structure is freely allowed to slide on the cage in order to ensure that the motion of the robot is not restricted in its general direction of walking. The off board processing unit is connected to the drives of the joints via ETHERCAT. The desired joint angles and velocities are generated by the off board processing unit in real time using the optimal gait parameters α^* from the gait optimization, and sent to the local controller at the rate of 1 kHz. The speed of the treadmill can be changed from its control panel, and the actual speed of the treadmill is measured by an encoder, the readings are updated and sent to the off board processing unit at the rate of 1 kHz.

Nominal Gait Generation. First, we use the exact same optimization formulation in (24) to generate a nominal gait off-line. In this case, we run the optimization from a set of random initial guesses (of the decision variables). The desired walking speed of the nominal gait is chosen to be 0.65 m/s. The offline optimization, which runs on a laptop computer with an Intel Core i7-3820QM processor (2.7 GHz) and 12 GB of RAM, converges to an optimal solution

¹For constraints (C1), (C2), and (C4), we use their modified formulations in (C1-a) – (C1-d), (C2-a), and (C4-a)–(C4-f) respectively.

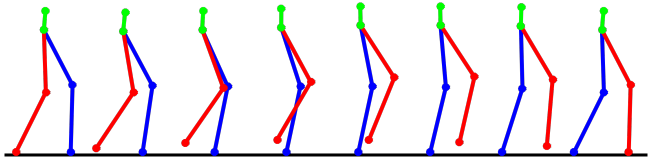


Fig. 5: Snapshots of the nominal gait in simulation.

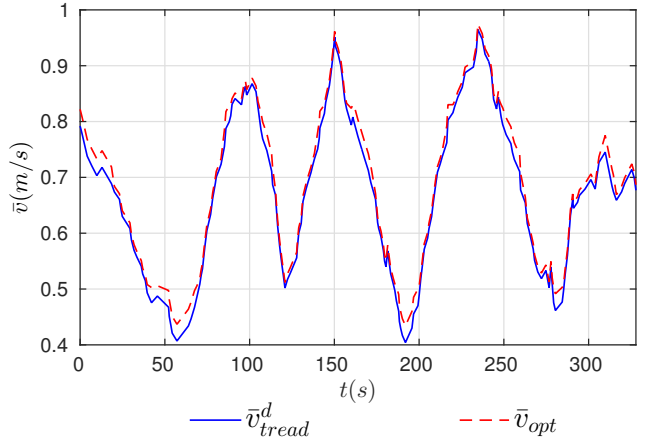


Fig. 6: The tracking of varied treadmill speed, \bar{v}_{tread}^d . The dashed line represents the speed, \bar{v}_{opt} , of the optimized gait.

successfully with an average CPU time of 9.5 seconds. Fig. 5 shows a series of snapshots of the nominal gait during one step in simulation.

Performance of Online Optimization. The measured treadmill speed serves as the desired speed \bar{v}^d in (24) and is published to a ROS message at the beginning of every step. Once the online gait optimizer, which runs on the same laptop computer, receives a new message from the ROS message, the optimizer runs a new optimization subject to the new desired walking speed if the difference between the updated speed and previously optimized speed is greater than a certain threshold. In particular, we pick both the threshold and the δ in (OC1) to be 0.01. Once the optimization converges, new gait parameters are sent to the off board processing unit immediately and applied to the gait controller at the beginning of the next robotic step.

For the experimental results reported in this paper, we started from the nominal gait and then changed the treadmill speed from its control panel within a range from 0.43 m/s to 0.97 m/s. The treadmill speed was slowed down and speeded up multiple times, as the blue line shown in Fig. 6. The dashed red line in Fig. 6 showed that the online optimizer generates new gaits that closely tracked the desired walking speed.

In order to achieve faster convergence, we enabled the warm start feature of the optimizer in IPOPT where we used the results from the previous optimization as the initial guess for the next optimization. Further we provided the exact Hessian of the problem using the analytical second order derivatives of all constraints and cost function instead of the Quasi-Newton approximation of the Hessian. By doing so, the optimizations converged faster and more reliably. Fig. 8 shows the histogram figures of the CPU time spent and

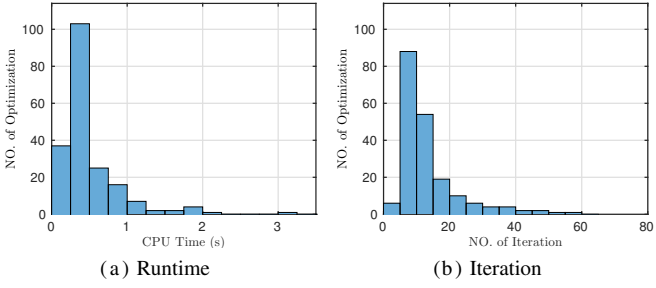


Fig. 7: The histogram plots of total 198 gait optimizations.

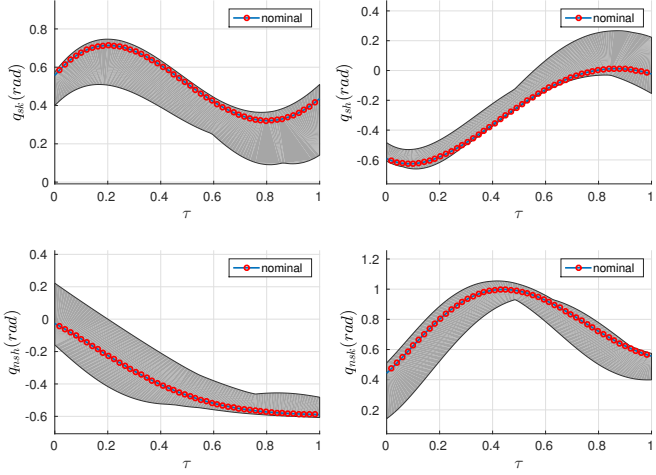


Fig. 8: The gray areas represent desired outputs of optimal gaits at different walking speeds generated by the online optimizer. The blue lines with red circles show the desired outputs of the nominal gait.

total number of iterations of each optimization. The average CPU time spent of the total 198 gait optimizations during the experiment of 328 seconds is 0.4964 second, which is less than the average time of one step. There are only two occasions when the optimizer ran for more than 2 seconds. Furthermore, the online optimizer converged successfully to an optimal solution in all occurrences within the maximum allowed iterations of 100. In fact, the average number of iterations is just about 13 with the maximum number being 67. The video demonstration of this experiment can be found in [1].

The performances of the online gait optimization when providing the exact and Quasi-Newton approximation of the

TABLE I: Performance comparison of online gait optimization with different methods of computing the Hessian (Total number of optimizations is: 198).

Method	CPU Time (sec)		NO. of Iteration	
	Average	Std.	Average	Std.
Exact Hessian	0.4954	0.3997	13.1414	10.13
Quasi-Newton	0.8927	0.8749	44.5657	36.60

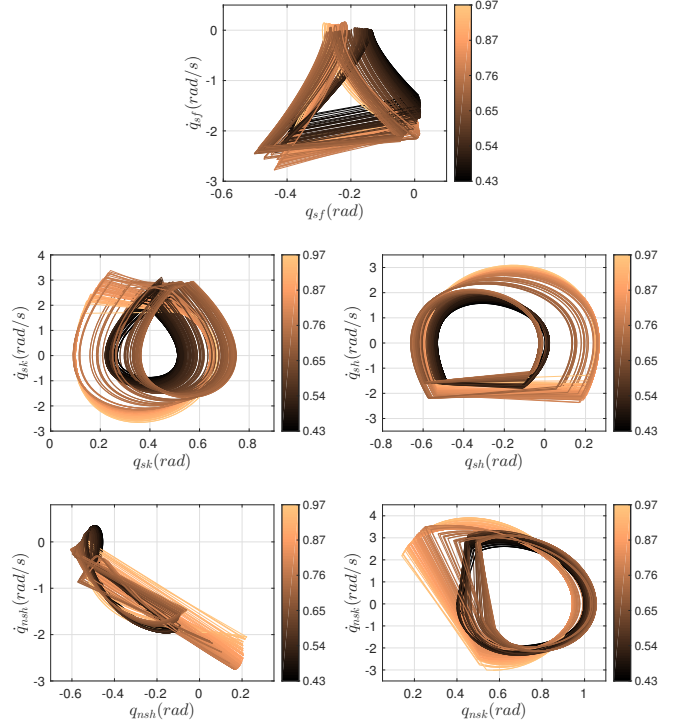


Fig. 9: Phase portraits of optimal gaits at different walking speeds generated by the online optimizer. The color bar indicates the speed of the gaits, where darker lines represent slower speeds and lighter lines represent faster speeds.

Hessian are also studied. The comparison results are shown in Table I, in which the optimizer spent more time and required more iterations to converge. Further, in 50 of total 198 occurrences when using the Quasi-Newton approximation, the optimization stalled at an almost feasible solution, which is indicated as the “Restoration Failed” in IPOPT outputs². These failures do not occur when we were using the exact Hessian for the problem.

Gait Performance. With the proper objective-orientated constraints presented in Sec. IV, all gaits generated from the online optimizer are physically realizable on the DURUS-2D hardware. Fig. 10 shows the snapshots of the gaits during the speed regulated walking experiment. Fig. 8 shows the range of desired outputs of all gaits generated. These gray areas are then compared to the desired outputs of the nominal gait, which shows very good similarities. Fig. 9 shows the phase portraits of robot joints for all gaits generated, where darker lines represent the slower gaits and lighter lines represent the faster gaits. It can be noted that each gait produces periodic orbits for the robot joints. Also, the size of the orbits is expanded when the speed of the robot is increased, which shows that the optimizer generated gaits with faster joint velocities and wider joints movements as the speed increased.

²<http://www.coin-or.org/Ipopt/documentation/node35.html>

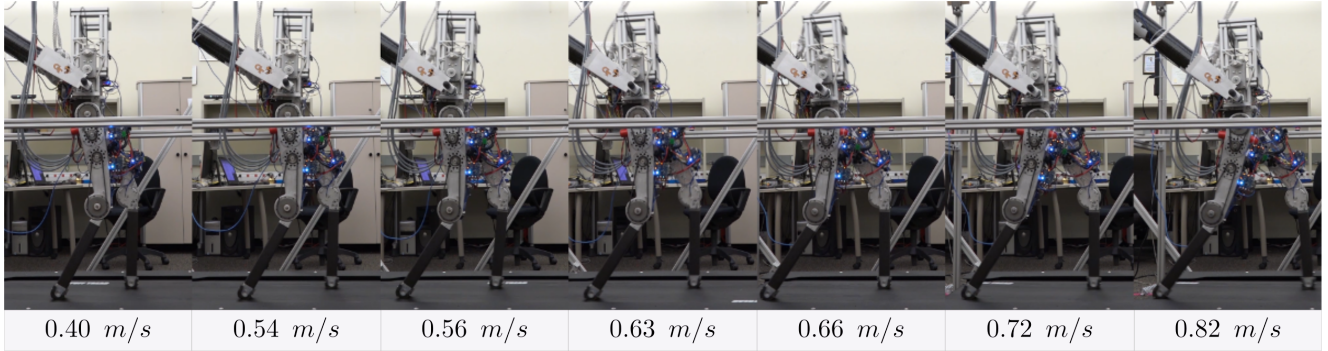


Fig. 10: Snapshots of optimal gaits generated from the online optimizer at different walking speeds.

VI. CONCLUSION

This paper presented an online gait optimization approach for generating dynamic locomotion on an underactuated robot under the hybrid zero dynamics framework. Building upon the theoretical foundation of HZD, this method optimizes the interactions of the full body dynamics of the robots hybrid system model, without restricting motions to simpler more-tractable dynamics (e.g., inverted pendulum models). More importantly, the utilization of the state-of-the-art pseudospectral method empowers a fast and reliable gait optimization method which is, for the first time, capable of generating HZD gaits online.

We experimentally validated the optimization method on a planar 5-link underactuated robot to generate gaits online subject to varying desired walking speeds. The online full body dynamics optimizer successfully optimized energy-efficient walking gaits in average of 0.5 seconds, while satisfying all dynamical and kinematics constraints.

REFERENCES

- [1] Online Hybrid Zero Dynamics Optimal Gait Generation Using Legendre Pseudospectral Optimization: <https://www.youtube.com/watch?v=pvH3c2G2Pj4>.
- [2] A. D. Ames. Human-inspired control of bipedal walking robots. *IEEE Transactions on Automatic Control*, 59(5):1115–1130, May 2014.
- [3] A. D. Ames, K. Galloway, K. Sreenath, and J. W. Grizzle. Rapidly exponentially stabilizing control lyapunov functions and hybrid zero dynamics. *IEEE Transactions on Automatic Control (TAC)*, 59(4):876–891, April 2014.
- [4] B. G. Buss, A. Ramezani, K. Akbari Hamed, K. S. Griffin, B. A. Galloway, and J. W. Grizzle. Preliminary Walking Experiments with Underactuated 3D Bipedal Robot MARLO. In *Intelligent Robots and Systems (IROS 2014)*, pages 2529–2536. IEEE, 2014.
- [5] E. A. Cousineau and A. D. Ames. Realizing underactuated bipedal walking with torque controllers via the ideal model resolved motion method. In *IEEE International Conference on Robotics and Automation*, 2015.
- [6] Hongkai Dai, Andrés Valenzuela, and Russ Tedrake. Whole-body motion planning with centroidal dynamics and full kinematics. In *2014 14th IEEE-RAS International Conference on Humanoid Robots (Humanoids)*, pages 295–302. IEEE, 2014.
- [7] Gamal Elnagar, Mohammad Kazemi, and Mohsen Razzaghi. The pseudospectral legendre method for discretizing optimal control problems. *Automatic Control, IEEE Transactions on*, 40(10):1793–1796, 1995.
- [8] Divya Garg. *Advances in global pseudospectral methods for optimal control*. PhD thesis, University of Florida, 2011.
- [9] Qi Gong, Wei Kang, and M. I. Ross. A pseudospectral method for the optimal control of constrained feedback linearizable systems. *Automatic Control, IEEE Transactions on*, 51(7):1115–1129, 2006.
- [10] J. W. Grizzle, C. Chevallereau, R. W. Sinnet, and A. D. Ames. Models, feedback control, and open problems of 3D bipedal robotic walking. *Automatica*, 50(8):1955 – 1988, 2014.
- [11] K. A. Hamed and J. W. Grizzle. Robust event-based stabilization of periodic orbits for hybrid systems: Application to an underactuated 3D bipedal robot. In *American Control Conference (ACC), 2013*, pages 6206–6212, June 2013.
- [12] A. Hereid, E. A. Cousineau, C. M. Hubicki, and A. D. Ames. 3D dynamic walking with underactuated humanoid robots: A direct collocation framework for optimizing hybrid zero dynamics. In *International Conference on Robotics and Automation*. IEEE, 2016.
- [13] Y. Hurmuzlu and D. B. Marghitu. Rigid body collisions of planar kinematic chains with multiple contact points. *The International Journal of Robotics Research*, 13(1):82–92, 1994.
- [14] S Kajita, F Kanehiro, K Kaneko, K Yokoi, and H Hirukawa. The 3d linear inverted pendulum model: a simple modeling for a biped walking pattern generation. In *Proceedings of the IEEE/RSJ International Conference on Intelligent Robots and Systems*, pages 239–246, 2001.
- [15] S. Kajita et al. Biped walking pattern generation by using preview control of zero-moment point. In *IEEE International Conference on Robotics and Automation*, volume 2, pages 1620–1626. IEEE, 2003.
- [16] Igor Mordatch, Kendall Lowrey, and Emanuel Todorov. Ensemblecio: Full-body dynamic motion planning that transfers to physical humanoids. In *2015 IEEE/RSJ International Conference on Intelligent Robots and Systems (IROS)*, pages 5307–5314. IEEE, 2015.
- [17] Ill W. Park, Jung Y. Kim, Jungho Lee, and Jun H. Oh. Online free walking trajectory generation for biped humanoid robot KHR-3(HUBO). *Proceedings - IEEE International Conference on Robotics and Automation*, 2006(May):1231–1236, 2006.
- [18] Michael Posa, Cecilia Cantu, and Russ Tedrake. A direct method for trajectory optimization of rigid bodies through contact. *The International Journal of Robotics Research*, 33(1):69–81, 2014.
- [19] M. J. Powell, A. Hereid, and A. D. Ames. Speed regulation in 3d robotic walking through motion transitions between human-inspired partial hybrid zero dynamics. In *IEEE International Conference on Robotics and Automation*, pages 4803–4810. IEEE, 2013.
- [20] I Michael Ross and Fariba Fahroo. A unified computational framework for real-time optimal control. In *Proceedings 42nd IEEE Conference on Decision and Control*, volume 3, pages 2210–2215. IEEE, 2003.
- [21] K. Sreenath, H. Park, I. Pouliquen, and J. W. Grizzle. A compliant hybrid zero dynamics controller for stable, efficient and fast bipedal walking on MABEL. *The International Journal of Robotics Research*, 30(9):1170–1193, 2011.
- [22] Miomir Vukobratović and Branislav Borovac. Zero-moment point—thirty five years of its life. *International Journal of Humanoid Robotics*, 1(01):157–173, 2004.
- [23] A. Wächter and L. T. Biegler. On the implementation of an interior-point filter line-search algorithm for large-scale nonlinear programming. *Mathematical programming*, 106(1):25–57, 2006.
- [24] E. R. Westervelt, J. W. Grizzle, C. Chevallereau, J. H. Choi, and B. Morris. *Feedback control of dynamic bipedal robot locomotion*. CRC press Boca Raton, 2007.
- [25] Hui-Hua Zhao, Wen-Loong Ma, Michael B Zeagler, and Aaron D Ames. Human-inspired multi-contact locomotion with amber2. In *IC-CPS'14: ACM/IEEE 5th International Conference on Cyber-Physical Systems (with CPS Week 2014)*, pages 199–210. IEEE Computer Society, 2014.